Aspects of Higgs searches in CP-violating MSSM at the Large Hadron Collider

Priyotosh Bandyopadhyay
Korea Institute for Advanced Study, Seoul

September 10, 2011
2011 IPMU-YITP School and Workshop on Monte Carlo Tools for LHC , Kyoto University, Kyoto, Japan

Work done with Prof. Amitava Datta, Prof. AseshKrishna Datta, Prof. Biswarup Mukhopadhyaya, Prof. Katri Huitu

Phys.Rev. D78 (2008) 015017, JHEP 1108:016,2011, arXiv:1106.5108 [hep-ph]

Plan

1. Higgs sector CP-volation as loop effects in MSSM
2. Constraints
3. Review
4. Phenomenology at the LHC
    - Associated Higgs production
    - Pair Production
    - Higgs production in CPV-cascade
5. Conclusion

Sources of CP violating phases in MSSM

- In SM we have two CP-violating phases, θ_{QCD} and δ_{CKM}.
- Unlike SM, MSSM is the source of many other CP-violating phases.
- The one which appears in the μ term of the superpotential is,
  $$W \supset \mu H_u \cdot H_d$$
- Those appear in the soft-SUSY breaking terms are as follows:

$$
\begin{aligned}
-\mathcal{L}_{\mathrm{soft}} \supset \; & \frac{1}{2}(M_3 \widetilde{g}\widetilde{g} + M_2 \widetilde{W}\widetilde{W} + M_1 \widetilde{B}\widetilde{B} + \mathrm{h.c.}) \\
& + \widetilde{Q}^\dagger \mathbf{M}^2_{\widetilde{\mathbf{Q}}} \widetilde{Q} + \widetilde{L}^\dagger \mathbf{M}^2_{\widetilde{\mathbf{L}}} \widetilde{L} + \widetilde{u}^*_R \mathbf{M}^2_{\widetilde{\mathbf{u}}} \widetilde{u}_R + \widetilde{d}^*_R \mathbf{M}^2_{\widetilde{\mathbf{d}}} \widetilde{d}_R + \widetilde{e}^*_R \mathbf{M}^2_{\widetilde{\mathbf{e}}} \widetilde{e}_R \\
& - m_1^2 H_d^* H_d - m_2^2 H_u^* H_u - (m_{12}^2 H_u H_d + \mathrm{h.c.}) \\
& + (\widetilde{u}^*_R \mathbf{A_u} \widetilde{Q} H_u - \widetilde{d}^*_R \mathbf{A_d} \widetilde{Q} H_d - \widetilde{e}^*_R \mathbf{A_e} \widetilde{L} H_d + \mathrm{h.c.})
\end{aligned}
$$

CP violating phases in MSSM

- But all the phases are not independent.
- Physical ovservables depend on the two combinations:

$$\mathrm{Arg}(M_i\,\mu\,(m_{12}^2)^*)\,, \quad \mathrm{Arg}(A_f\,\mu\,(m_{12}^2)^*)\,,$$

with $i = 1-3$ and $f = e, \mu, \tau; u, c, t, d, s, b$.

- Most relevant CP phases pertinent to the Higgs sector:

$$\Phi_i \equiv \mathrm{Arg}(M_i)\,; \quad \Phi_{A_{f_3}} \equiv \mathrm{Arg}(A_{f_3})\,,$$

with $f_3 = \tau, t, b$.

CP violation in the Higgs sector

- Even though CP can be violated explicitely, it does not affect the Higgs sector at the tree-level.
- CP violation in the Higgs potential of the MSSM leads to mixing terms between the CP-even and CP-odd Higgs fields. more

  Pilaftsis, etal; 88,98
- In the weak basis (G^0, a, ϕ_1, ϕ_2), the neutral Higgs-boson mass matrix $\mathcal{M}_0^2$ may be cast into the form

$$\mathcal{M}_0^2 = \begin{pmatrix} \widehat{\mathcal{M}}_P^2 & \mathcal{M}_{PS}^2 \\ \mathcal{M}_{SP}^2 & \mathcal{M}_S^2 \end{pmatrix}$$

where,

$$\widehat{\mathcal{M}}_P^2 \Rightarrow \begin{pmatrix} G^0 \\ a \end{pmatrix} \leftrightarrow \begin{pmatrix} G^0 \\ a \end{pmatrix} \qquad \mathcal{M}_S^2 \Rightarrow \begin{pmatrix} \phi_1 \\ \phi_2 \end{pmatrix} \leftrightarrow \begin{pmatrix} \phi_1 \\ \phi_2 \end{pmatrix}$$

$$\mathcal{M}_{PS}^2 = (\mathcal{M}_{SP}^2)^T \qquad \Rightarrow \begin{pmatrix} G^0 \\ a \end{pmatrix} \leftrightarrow \begin{pmatrix} \phi_1 \\ \phi_2 \end{pmatrix}$$

- The mixing term :

$$\mathcal{M}^2_{SP} = -\frac{T_a}{v}\begin{pmatrix} s_\beta & c_\beta \\ -c_\beta & s_\beta \end{pmatrix} \simeq \mathcal{O}\left(\frac{m_t^4}{v^2}\frac{|\mu||A_t|}{32\pi^2 M^2_{\rm SUSY}}\right)\sin\phi_{\rm CP}$$

where,

$$\phi_{\rm CP} = \arg(A_t\mu) + \xi \quad M^2_{\rm SUSY} = \frac{1}{2}\left(m^2_{\tilde{t}_1} + m^2_{\tilde{t}_2}\right)$$

- CP-phases of gnuino mass parameter also contribute through the threshold corrections $\sim f(M^*\mu^*)$.

CP violation in MSSM contd.

- G_0 is massless: Doesn't mix with other neutral fields.
- $\mathcal{M}_0^2$ reduces to a (3×3)-dimensional matrix, $\mathcal{M}_N^2$ in the basis (a, ϕ_1, ϕ_2).
- $\mathcal{M}_N^2$ is symmetric, we can diagonalize it by means of an orthogonal rotation O as follows:

$$O^T \, \mathcal{M}_N^2 \, O \;=\; \mathrm{diag}\,(M_{h_3}^2,\; M_{h_2}^2,\; M_{h_1}^2)\;.$$

- Where,

$$M_{h_1} \;\leq M_{h_2} \;\leq M_{h_3}\;.$$

- Do not have any definite CP properties.

The CPX scenario

- The mixing become significant when $\mathrm{Im}(\mu A_t/M^2_{SUSY})$ is large.
- Motivated by this following CP-violating benchmark scenario CPX was introduced in the literature.
  Carena,Pilaftsis, Ellis, Wagner

$$
\begin{aligned}
&M_{\tilde{Q}_3} = M_{\tilde{U}_3} = M_{\tilde{D}_3} = M_{\tilde{L}_3} = M_{\tilde{E}_3} = M_{\mathrm{SUSY}}\,, \\
&|\mu| = 4\, M_{\mathrm{SUSY}}\,, \quad |A_{t,b,\tau}| = 2\, M_{\mathrm{SUSY}}\,, \quad |M_3| = 1\ \ \mathrm{TeV}.
\end{aligned}
$$

- The parameter $\tan\beta$, $M_{H^\pm}$, and M_{SUSY} can be varied.
- For CP phases, $\Phi_A = \Phi_{A_t} = \Phi_{A_b} = \Phi_{A_\tau}$, we have two physical phases to vary: Φ_A and $\Phi_3 = \mathrm{Arg}(M_3)$.
- Special case:

$$
\begin{aligned}
&M_{SUSY} = 500\ \mathrm{GeV}, \quad \Phi_A = \Phi_{M_3} = 90^\circ \\
&M_2 = 2M_1 = 200\ \mathrm{GeV}, \quad \tan\beta = 5-10
\end{aligned}
$$

The Experimental constraints

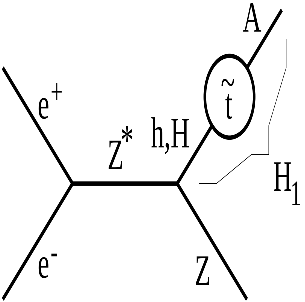

- $h_1 \sim$ CP-odd.
- As $h_1 \simeq A \Rightarrow Z - Z - h_1$ coupling goes down.
  $\Rightarrow$ could not probe the channel in the CPX scenario at LEP.

The Experimental constraints

- LEP put a lower bound on SM Higgs: $m_H \geq 114.4$ GeV.
- Similar bound on CPC MSSM Higgs: $m_h \geq 92.9$ GeV.
- The 'LEP hole' in CPX scenario

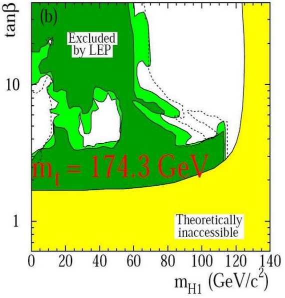

- Tevatron also confirms 'LEP hole' for a small region of parameter space.

  Wagner et al., arxiv:0911.0034v2[hep-ph]

- $Z - Z - h_1$ coupling goes down.
  $\Rightarrow$ can not probe the CPX.
  $g_{t\bar{t}h_1}$ also goes down.
- Need to find out a channel to probe CPX.
- Sum rule:

$$g^2_{h_i VV} + \mid g_{h_i H^- W^+} \mid^2 = 1$$

$$g^2_{h_i VV} \downarrow \quad \Rightarrow \quad g_{h_i H^- W^+} \uparrow$$

- New channel: $pp \to H^+ h_1 \to h_1 h_1 W^+ \to b\bar{b}b\bar{b}l\nu$
  15-45 events predicted at 10-30 fb^{-1} integrated luminosity.
  Moretti, Gosh, Eur. Phys. J. C42, 341, (2005)

CPX:"LEP-hole" and Earlier works

- New channel: $pp \to t\bar{t} + X \to bbbbqql\nu$
  with $3 - b$ tagged, predicts $\sim 1000 - 5000$ events at 30 fb^{-1}.
  Gosh, Roy and Godbole, Phys. Lett. B628,131,(2005)
- $p\bar{p}/pp \to Wh_2 \to 4j + l + \not{p}_T$
  $\Rightarrow$it is very hard to observe this signature at the Tevatron, even with 20fb^{-1} of data
  one has to wait for LHC with 20 to 50fb^{-1} of data to probe the 'LEP hole'.
  A. Datta, M. Dress, S.P. Das, arXiv:0809:2209[hep-ph], Phys. Rev. D 83, 035003(2011)

- As $m_{\tilde{t}_1} \downarrow$ and $g_{\tilde{t}_1 \tilde{t}_1^* h_1} \uparrow$
- Low $m_{h_1}(\leq 60$ GeV)
- $\Rightarrow \tilde{t}_1 \tilde{t}_1^* h_1$ can be promising
  AD, BM and PB, *Phys.Rev. D78 (2008) 015017*
- Look at the status in different points in the "LEP hole" in $m_{h_1} - \tan\beta$ plane

- With the choice of $\tan\beta$=5 and $m_{H^\pm}$=130 we get $m_{h_1} = 48.9$ GeV and $m_{\tilde{t}_1} = 322.0$ GeV $\Rightarrow \sigma_{\tilde{t}_1 \tilde{t}_1^* h_1} = 440$ fb.
- Then h_1 mainly decays to $b\bar{b}$ (Br($h_1 \to b\bar{b}$)=0.91)
- $\tilde{t}_1 \to b\chi_1^+ (t\chi_1^0) \to bW^+\chi_1^0 \to b\ell^+\nu_\ell\chi_1^0$
- $\Rightarrow$ parton level signal:
  4-b partons + dilepton + $\not{p}_T$
- with ISR/FSR taken into account the final signal becomes:
  5-jets ($\geq 3b$-jets) + dilepton + $\not{p}_T$

Three Scenarios

- The CPV-SUSY : $pp \to \tilde{t}_1 \tilde{t}_1^* h_1, t\bar{t}h_{2,3}$ and $pp \to \tilde{g}\tilde{g}$
  where m_{h_1} could be as light as 50 GeV

- (CPC-SUSY):$pp \to t\bar{t}h$ and $\tilde{g}\tilde{g}$,
  where the appropriate LEP bound hold for m_h

- SM: $pp \to t\bar{t}H$,
  where $m_H > 114.4$ GeV.

- common background: The SM contributions coming from
  $pp \to t\bar{t}, t\bar{t}Z, t\bar{t}b\bar{b}$

Relevant distributions

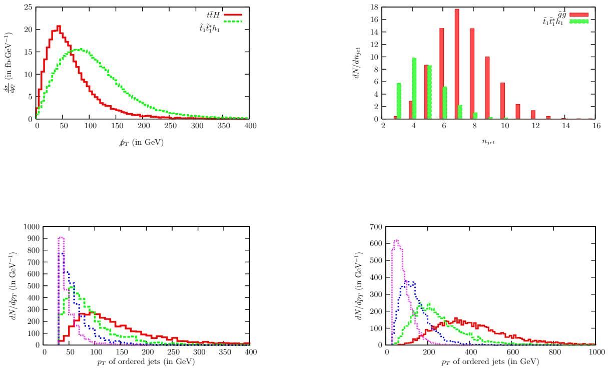

Figure: p_T^{jet} distribution of $\tilde{t}_1\tilde{t}_1^* h_1$ and $\tilde{g}\tilde{g}$.

Special cuts

- $\not{p}_T \geq 110$ GeV kills the SM backgrounds
- $n_{jet} \leq 5$ was imposed to get rid of $\tilde{g}\tilde{g}$, which is not sufficient
- An upper p_T^{jet} cut, i.e, $p_T^{jet} \leq 300$ GeV kills ths strong background ▸ more

Results

- Special cuts + Basic cuts $\Rightarrow$ Optimize the signal
- Specifically, CPX signal has enough strength ($\sim$ 14 σ) over Common Background at $\mathcal{L}$=30fb^{-1} more
- After upper p_T^{jet} cut, we got rid of strong production to distinguish CPX from other scenarios
- With these: CPX signal size(7.2 σ) is still larger than more CPC or SM
- We have taken an overall systematics and statistical uncertainty around 15%
- After the signal can be more than Common Background at $\sim$ 6.2σ level

Higgs pair production

- Unlike other processes Higgs pair production channels are clean
- We probe $pp \to h_1 h_{2,3}$ at the LHC.
- In CPX scenario there are points where the heavier Higgses decay as:$h_{3,2} \to Z, h_1$.
  $\Rightarrow\ pp \to 4b + 2l$ signal topology.

KH, PB, arXiv:1106.5108 [hep-ph]

Higgs pair production

- We vary ϕ_{A_t}, $\tan_\beta$ and $m_{H^\pm}$ to select following benchmark points

Parameters	BP1	BP2	BP3
$\tan\beta$	5	5	5
ϕ_{A_t}	112	122	124
$m_{H^\pm}$	146	155	154
m_{h_1}	31.0	30.8	12.6
m_{h_2}	117.3	124.1	124.2
m_{h_3}	146.1	152.8	151.5

Table: Benchmark points within the LEP-hole in m_{h_1}-$\tan\beta$ plane.

Higgs pair production

- The corresponding cross-sections are

Benchmark Points	$\sigma(h_i h_3)$ in fb	$\sigma(h_1 h_2)$ in fb
BP1	226	285
BP2	206	323
BP3	248	7929

- Enhancement in cross-section happens for BP3. ▸ more

Relevant distributions

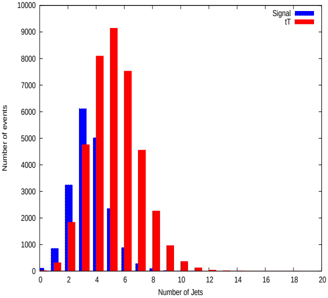

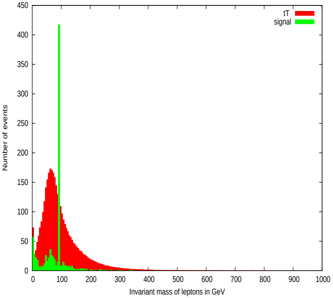

- Jet multiplicity distribution with ISR, FSR and MI
  $\Rightarrow$ lower numbers jet in the final state for signal.
- Lepton invariant mass distribution
  $\Rightarrow$ peaked at the Z mass for the case of signal.

Signal and Backgrounds

Final state analysed:

$$n_{jet} \leq 4(b - \mathrm{jet} \geq 3) + l \geq 2(\mathrm{OSD} \geq 1) + \not{p}_{\mathrm{T}} \leq 20$$

- Cuts: $p_T^{j_1} \leq 75\mathrm{GeV}, \mathrm{p_T^{j_2}} \leq 50\mathrm{GeV}$
- $M_{eff} \leq 200\mathrm{GeV} + |\mathrm{M_{ll}} - 90| \leq 3\mathrm{GeV}$

Backgrounds: $t\bar{t}$, $t\bar{t}Z$, $t\bar{t}b\bar{b}$

Higgs pair production

- 20 fb^{-1} integrated lumnosity is enough to get 5σ significance.
- At BP3 due to enhancement of $h_1 - h_2 - h_3$ coupling leads to increase of $h_1 h_2$ production cross-section
  $\Rightarrow$ possible reach with early data of LHC,
  $\Rightarrow$ have a possibility to probe the Higgs potential at those points.
- Being clean in terms of jets, the reconstruction of Higgs mass peak is quite possible

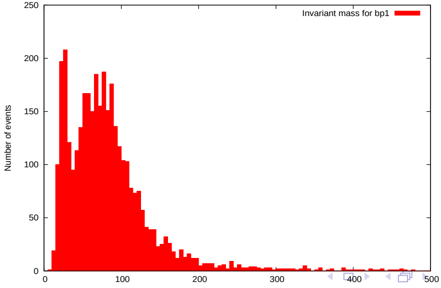

- Strongly interacting particles are copiously produced at the LHC.
- Mass spectrum (in GeV) in CPX scenario with $\tan\beta$=5 and $m_{H^\pm}$=130 GeV, i.e. BP1.

m_{h_1}	m_{h_2}	m_{h_3}
39.8	104.7	137.1

$m_{\tilde{t}_1}$	$m_{\tilde{t}_2}$	$m_{\tilde{b}_1}$	$m_{\tilde{b}_2}$	$m_{\chi_1^0}$	$m_{\chi_2^0}$	$m_{\chi_1^\pm}$
317.6	668.2	475.9	526.6	99.6	198.4	198.4

- The cross sections (in fb): computed with CalcHEP (interfaced with the program CPSuperH)

$\sigma_{\tilde{t}_1\tilde{t}_1^*}$	$\sigma_{\tilde{b}_1\tilde{b}_1^*}$	$\sigma_{\tilde{t}_2\tilde{t}_2^*}$	$\sigma_{\tilde{b}_2\tilde{b}_2^*}$	$\sigma_{\tilde{t}_1\tilde{t}_2}$	$\sigma_{\tilde{b}_1\tilde{b}_2}$	$\sigma_{\tilde{t}_i\tilde{b}_j}$	$\sigma_{\tilde{g}\tilde{g}}$
2861	323.3	4	178.5	8	0.6	7	135

$\tilde{t}_1 \tilde{t}_1^*$ cascade

$\mathrm{Br}(\tilde{t}_1 \to b\chi_1^+)$	$\mathrm{Br}(\tilde{t}_1 \to t\chi_1^0)$
0.81	0.19

- $Br(H^\pm \to h_1 W^\pm) = 0.84 \quad \Rightarrow$ leads to non-trivial signatures
- $\tilde{t}_1 \tilde{t}_1{}^* \to t\bar{t}\chi_1^0\chi_1^0 \to b\bar{b}H^+H^-\chi_1^0\chi_1^0 \to b\bar{b}W^+W^-h_1h_1\chi_1^0\chi_1^0$
- But $\mathrm{Br}(t \to bH^+) \simeq 0.011$
  $\Rightarrow \mathrm{Br}(\tilde{t}_1\tilde{t}_1^* \to b\bar{b}H^+H^-\chi_1^0\chi_1^0) \simeq 5 \times 10^{-6}$

$\tilde{t}_1 \tilde{t}_1^*$ cascade

- If one of the $\tilde{t}_1$ decays via $\tilde{t}_1 \to b\chi_1^+$ and this gives rise to the following signal signal topologies.

$$\tilde{t}_1 \tilde{t}_1{}^* \to t\bar{b}\chi_1^0\chi_1^- \to b\bar{b}H^+W^-\chi_1^0\chi_1^0 \to b\bar{b}h_1W^+W^-\chi_1^0\chi_1^0$$

$$\to 4b + 4(non - b)jet + \not{p}_T$$

$$\to 4b + 1(non - b)jet + 1\ell + \not{p}_T$$

$$\to 4b + OSD + \not{p}_T$$

$\tilde{b}_1\tilde{b}_1^*$ cascade

$\mathrm{Br}(\tilde{b}_1 \to \tilde{t}_1 H^-)$	$\mathrm{Br}(\tilde{b}_1 \to \tilde{t}_1 W^-)$
0.77	0.12

- $\tilde{b}_1 \to \tilde{t}_1 H^-$ is very large. $\Rightarrow$ both the $\tilde{b}_1$s can decay in that mode.
- $H^\pm \to h_1 W^\pm$ is also large as this mode is open here.
- Depending on the decay mode of w we can have the following final states.

$$pp \to \tilde{b}_1\tilde{b}_1{}^* \to \tilde{t}_1\tilde{t}_1{}^* H^+H^- \to b\bar{b}W^+W^-W^+W^-h_1h_1 + \not{p}_T$$

$$\to 6b + LSD + 4(non-b)jet + \not{p}_T$$

$$\to 6b + 3\ell + 2(non-b)jet + \not{p}_T$$

$$\to 6b + 4\ell + \not{p}_T$$

Contribution of $\tilde{g}\tilde{g}$cascade

$\text{Br}(\tilde{g} \to b\tilde{b}_1)$	$\text{Br}(\tilde{g} \to b\tilde{b}_2)$	$\text{Br}(\tilde{g} \to t\tilde{t}_1)$	$\text{Br}(\tilde{g} \to t\tilde{t}_2)$
0.28	0.24	0.32	0.16

- $\tilde{g}$ decays to $t\tilde{t}_1$ $b\tilde{b}_1$

  $\Rightarrow$ $\tilde{g}\tilde{g}$ also adds to the cross-section.

Possible parton level signals

Number of channels	Channels	Effective cross-sec (in fb)
1	$6b + LSD + 4(non-b)jet + \not{p}_T$	11.49
1	$6b + OSD + 4(non-b)jet + \not{p}_T$	22.98
2	$6b + 3\ell + 2(non-b)jet + \not{p}_T$	17.24
3	$6b + 4\ell + \not{p}_T$	8.62
4	$4b + 4(non-b)jet + \not{p}_T$	0.38
5	$4b + 1(non-b)jet + 1\ell + \not{p}_T$	0.18
6	$4b + OSD + \not{p}_T$	0.09

Table: Production cross sections (in fb) at lowest-order computed with `CalcHEP` interfaced with CPsuperH for different signal processes at the LHC in the CPX scenario and for the spectrum of BP1.

Set up for the numerical session

- Event generation: `CalcHEP` interfaced with`CPSuperH`.
- (Generated events + Relevant CPV-Brs) $\Rightarrow$ passed to PYTHIA(via SLHA).
- ISR/FSR, hadronization and jet formation: from PYTHIA.

Kinematical distributions

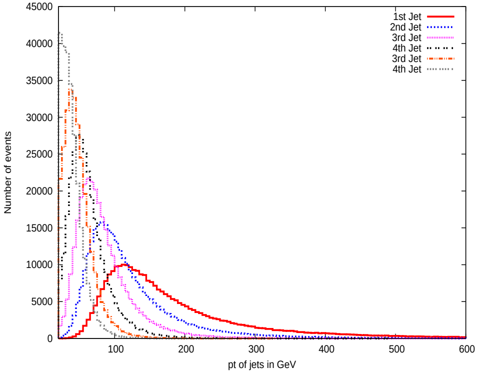

Figure: Ordered p_T^{jet} distributions in CPV-SUSY scenario for $\tilde{b}_1 \tilde{b}_1^*$

Backgrounds

- The main background for this case is $t\bar{t}$
- The other main SM backgrounds are $t\bar{t}Z$ and $t\bar{t}b\bar{b}$

Kinematical distributions

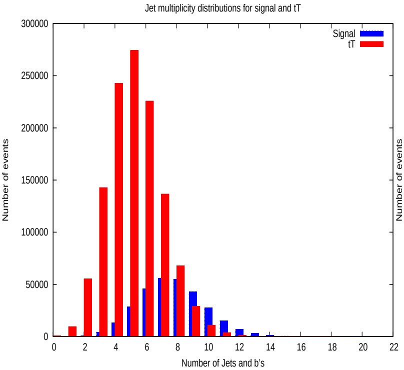

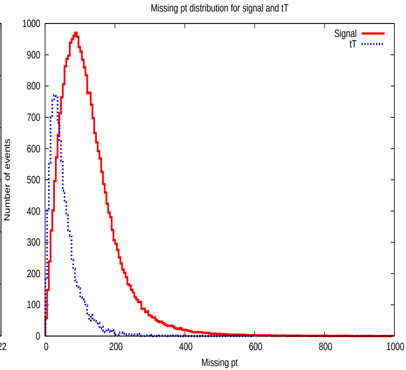

Figure: Ordered p_T^{jet} (left) and parton level b p_T distributions in CPV-SUSY scenario for $\tilde{b}_1 \tilde{b}_1^*$

Results and significance

- We analysed our signal for 9 different final states.
- We can get a significance $\geq 5 - 10\sigma$ for almost all the signal topologies at an integrated luminosity of 10 fb^{-1}.
- $\tilde{t}_1\tilde{t}_1^*$ contributes mostly for the low jet multiplicity signals.
- For the higher jet multiplicity the maximum contribution comes from $\tilde{g}\tilde{g}$
- $b - jets$ from the $\tilde{t}_1$ are of high p_T which are not there in SM backgrounds
- We demand $p_T^{j_1,J_2} \geq 100$ GeV.
- Implementation of these cuts increases the signal significance by 10-20%. more
- Depending on the scenarios, M_{SUSY} upto 1 TeV can be probed with an integrated luminosity of 10 fb^{-1} to 100 fb^{-1}.

THANK YOU

Results for signals

No.	Signal topology	$\tilde{b}_1\tilde{b}_1^*$	$\tilde{t}_1\tilde{t}_1^*$	$\tilde{g}\tilde{g}$
1	$n_{jet} \geq 8(b-\mathrm{jet} \geq 3) + l \geq 2 + \not{p}_T \geq 100$	10(5.6)	0.4(0.2)	53(52.8)
2	$n_{jet} \geq 8(b-\mathrm{jet} \geq 3) + l \geq 2(\mathrm{OSD} \geq 1) + \not{p}_T \geq 100$	7(3.9)	0.4(0.2)	37(36.7)
3	$n_{jet} \geq 8(b-\mathrm{jet} \geq 3) + l \geq 2(\mathrm{SSD} \geq 1) + \not{p}_T \geq 100$	4(2.2)	0(0)	23(22.1)
4	$n_{jet} \geq 8(b-\mathrm{jet} \geq 2) + l \geq 3 + \not{p}_T \geq 100$	2(1.1)	0(0)	8(8)
5	$n_{jet} \geq 8(b-\mathrm{jet} \geq 2) + l \geq 4 + \not{p}_T \geq 100$	0(0)	0(0)	1(0.8)
6	$n_{jet} \geq 8(b-\mathrm{jet} \geq 4) + l \geq 1 + \not{p}_T \geq 100$	3(1.5)	0(0)	34(33.2)
7	$n_{jet} \geq 4(b-\mathrm{jet} \geq 3) + l \geq 1 + \not{p}_T \geq 100$	116(63.6)	45(26.2)	283(279.3)
8	$n_{jet} \geq 4(b-\mathrm{jet} \geq 3) + l \geq 2(\mathrm{OSD} \geq 1) + \not{p}_T \geq 100$	21(9.7)	4(1.9)	54(52.9)
9	$n_{jet} \geq 8(b-\mathrm{jet} \geq 3) + \not{p}_T \geq 100$	149(96.3)	46(34.2)	499(498)

Table: Event rates for the CPX point(BP1) of an integrated luminosity of 10 fb^{-1}

- $p_T \geq 20$ GeV isolated leptons were demanded.

Results for background

No.	Signal topology	$t\bar{t}$	$t\bar{t}Z$	$t\bar{t}b\bar{b}$
1	$n_{jet} \geq 8(b-\mathrm{jet} \geq 3) + l \geq 2 + \not{p}_T \geq 100$	19(13)	0.33(0.27)	6.1(4.6)
2	$n_{jet} \geq 8(b-\mathrm{jet} \geq 3) + l \geq 2(\mathrm{OSD} \geq 1) + \not{p}_\mathrm{T} \geq 100$	17(12)	0.29(.23)	6.1(4.6)
3	$n_{jet} \geq 8(b-\mathrm{jet} \geq 3) + l \geq 2(\mathrm{SSD} \geq 1) + \not{p}_\mathrm{T} \geq 100$	3(1)	0.05(0.05)	0(0)
4	$n_{jet} \geq 8(b-\mathrm{jet} \geq 2) + l \geq 3 + \not{p}_T \geq 100$	0(0)	0.27(0.19)	0(0)
5	$n_{jet} \geq 8(b-\mathrm{jet} \geq 2) + l \geq 4 + \not{p}_T \geq 100$	0(0)	0.0(0.0)	0(0)
6	$n_{jet} \geq 8(b-\mathrm{jet} \geq 4) + l \geq 1 + \not{p}_T \geq 100$	5(5)	0.08(0.05)	2.6(2.4)
7	$n_{jet} \geq 4(b-\mathrm{jet} \geq 3) + l \geq 1 + \not{p}_T \geq 100$	1890(953)	22.6(13.21)	297.1 (170.4)
8	$n_{jet} \geq 4(b-\mathrm{jet} \geq 3) + l \geq 2(\mathrm{OSD} \geq 1) + \not{p}_\mathrm{T} \geq 100$	226(101)	2.7(1.4)	34.2(16.6)
9	$n_{jet} \geq 8(b-\mathrm{jet} \geq 3) + \not{p}_T \geq 100$	1109(784)	13.4(10.5)	252.3(185.6)

Table: Event rates for the CPX point(BP1) of an integrated luminosity of 10 fb^{-1}

- We extend this analysis to the other points of the 'LEP-hole'

Parameters	BP2	BP3	BP4
$\tan\beta$	4.0	4.0	7.0
$m_{H^\pm}$	140	135	125
m_{h_1} (GeV)	49.45	33.8	40.8

Table: Benchmark points within the LEP-hole in m_{h_1}-$\tan\beta$ plane.

- 5σ significance can be achieve with an integrated luminosity of 5-10 fb^{-1}.

Reach of CPX

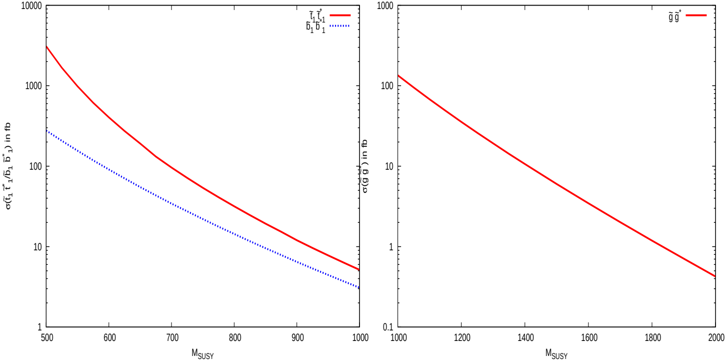

Figure: Cross-sec variation of with $M_{\rm SUSY}$ for $\tilde{t}_1\tilde{t}_1^*$, $\tilde{b}_1\tilde{b}^*$ (left) and $\tilde{g}\tilde{g}$ (right)

- When M_{SUSY} increases the 'LEP hole' almost vanishes, as the mixing term in the Higgs mass matrix, i.e., $M_{\mathrm{SP}} \simeq \frac{\mu^2 A}{M_{\mathrm{SUSY}}}$ goes to zero.
- **CPX1.0:**
  $\mu = 4M_{\mathrm{SUSY}}, \qquad |A| = 2M_{\mathrm{SUSY}}, \qquad |M_3| = 2M_{\mathrm{SUSY}}.$
  For this case with $M_{\mathrm{SUSY}} = 1\mathrm{TeV}$ the hole is still there near $m_{h_1} = 30 - 60$ GeV.
- **CPX0.5:**
  Where $M_{\mathrm{SUSY}} = 1$ TeV with all the other parameters kept in the as normal CPX. For this case the 'hole' is shifted to $m_{h_1} \geq 75$ GeV.
- For **CPX0.5** we still get 5σ significance at 10 fb^{-1}, whereas **CPX1.0** will require ≥ 100 fb^{-1}.

LEP-hole: Dependency on M_{SUSY}

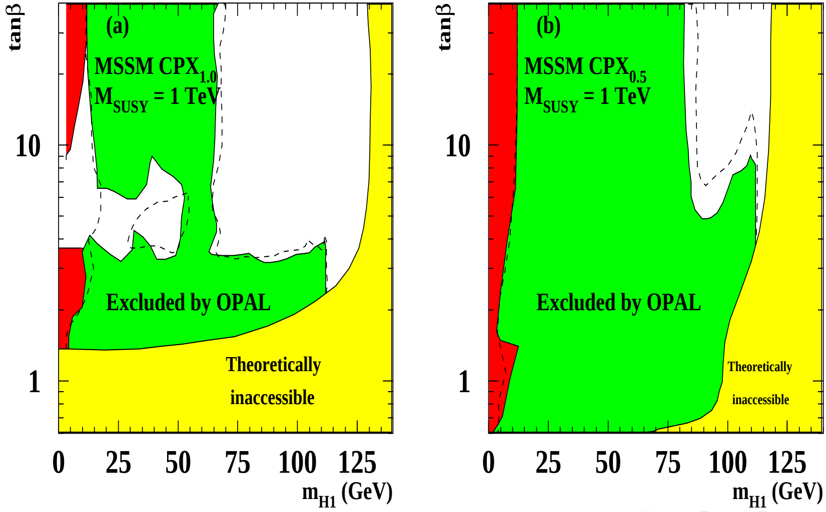

LEP-hole: Dependency on top mass

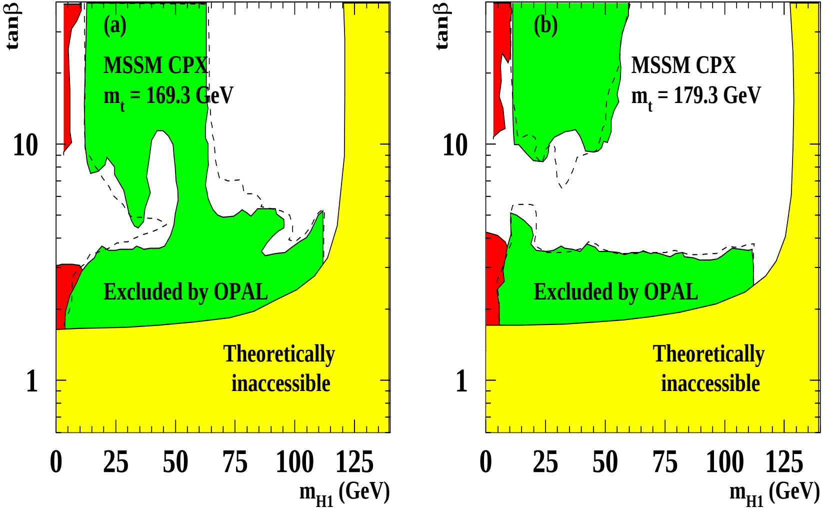

Current top mass: 172.7 $\pm$ 1.1(stat + syst) GeV (CDF, Winter conference 2011)

LHC: 0 lepton exclusion at $\sqrt{S} = 7$ TeV for mSUGRA

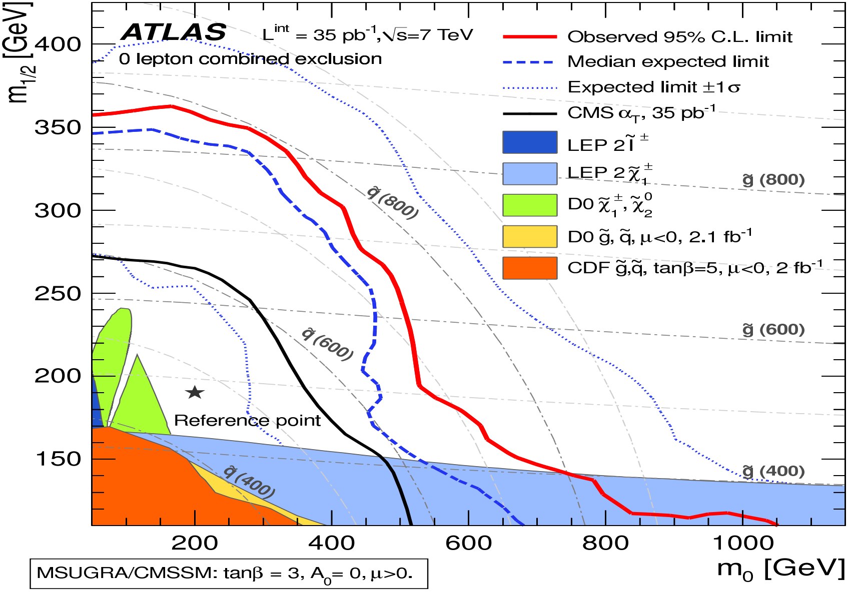

Signal & Events

- A suitable signal:
  dilepton $+ \leq 5$ *jets including three tagged b-jets* $+ \not{p}_T$

Scenarios	Processes	Hard Cross-sections in fb without cut	$\sigma \times \epsilon$ in fb without (with)upper p_T^{jet} cut	Events at $\mathcal{L}$=30 fb^{-1}
CPV SUSY	$\tilde{t}_1 \tilde{t}_1^* h_1$	440	0.5(0.38)	15(11)
	$t\bar{t}h_2$	197	0.23(0.16)	7(5)
	$t\bar{t}h_3$	135	0.23(0.17)	7(5)
	$\tilde{g}\tilde{g}$	134	0.70(0.167)	21(5)
CPC-SUSY	$t\bar{t}h$	330	0.33(0.27)	10(8)
	$CPC(\tilde{g}\tilde{g})$	134	0.70(0.167)	20(5)
SM	$SM(t\bar{t}H)$	340	0.33(0.27)	10(8)

back

Events: Common Background

Models	Processes	Hard Cross-sections in fb (without cut)	$\sigma \times \epsilon$ in fb without (with)upper p_T^{jet} cut	Events at $\mathcal{L}$=30 fb^{-1}
Common Background	$t\bar{t}$	3.7×10^5	0.1(0.1)	3(3)
	$t\bar{t}Z$	370	0.03(0.03)	1(1)
	$t\bar{t}b\bar{b}$	831	0.3(0.3)	9(9)

back

back

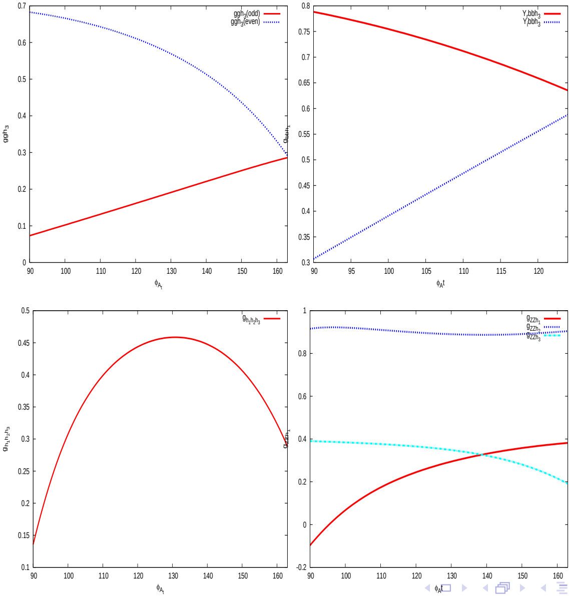

ggh3(odd)
ggh3(even)
ggh3
φAt
Yrbbh3
Yibbh3
gbbh1
φAt
gh1h2h3
φAt
gZZh1
gZZh2
gZZh3
φAt

CP violation in MSSM

- The Lagrangian describing the MSSM Higgs potential:

$$\begin{aligned}\mathcal{L}_V &= \mu_1^2(\Phi_1^\dagger\Phi_1) + \mu_2^2(\Phi_2^\dagger\Phi_2) + m_{12}^2(\Phi_1^\dagger\Phi_2) + m_{12}^{*2}(\Phi_2^\dagger\Phi_1) \\ &\quad + \lambda_1(\Phi_1^\dagger\Phi_1)^2 + \lambda_2(\Phi_2^\dagger\Phi_2)^2 + \lambda_3(\Phi_1^\dagger\Phi_1)(\Phi_2^\dagger\Phi_2) \\ &\quad + \lambda_4(\Phi_1^\dagger\Phi_2)(\Phi_2^\dagger\Phi_1)\end{aligned}$$

- The Higgs superfields are given by $H_u{=}\Phi_2$ and $H_d{=}\tilde{\Phi}_1 = i\tau_2\Phi_1^*$($\tau_2$ is the usual Pauli matrix)

CP violation in MSSM contd.

- $$\Phi_1 = \begin{pmatrix} \phi_1^+ \\ \frac{1}{\sqrt{2}}(v_1 + \phi_1 + ia_1) \end{pmatrix}, \Phi_2 = e^{i\xi} \begin{pmatrix} \phi_2^+ \\ \frac{1}{\sqrt{2}}(v_2 + \phi_2 + ia_2) \end{pmatrix}$$

  $v_1, v_2 \longrightarrow$ VEVs. of the Higgs doublets.
  $\xi \longrightarrow$ is their relative phase.

CP violation in MSSM contd.

- At the tree level, the parameters are given by

$$\mu_1^2 = -m_1^2 - |\mu|^2 \qquad \mu_2^2 = -m_2^2 - |\mu|^2 \qquad \lambda_1 = \lambda_2 = \frac{1}{8}(g_w^2 + g'^2)$$
$$\lambda_3 = -\frac{1}{4}(g_w^2 - g'^2), \qquad \lambda_4 = \frac{1}{2}g_w^2,$$

- Where, g_w, g' are the $\mathrm{SU}(2)_L$, $\mathrm{U}(1)_Y$ gauge couplings respectively and m_1^2, m_2^2 and m_{12}^2 are soft-SUSY-breaking parameters.

- These can be fixed by requiring the vanishing of the following tadpole parameters:

$$
\begin{aligned}
T_{\phi_1} &\equiv \langle \frac{\partial \mathcal{L}_V}{\partial \phi_1} \rangle = v_1 \Big[\mu_1^2 + \Re e(m_{12}^2 e^{i\xi}) \tan\beta - \frac{1}{2} M_Z^2 \cos 2\beta \Big] \\
T_{\phi_2} &\equiv \langle \frac{\partial \mathcal{L}_V}{\partial \phi_2} \rangle = v_2 \Big[\mu_2^2 + \Re e(m_{12}^2 e^{i\xi}) \cot\beta + \frac{1}{2} M_Z^2 \cos 2\beta \Big] \\
T_{a_1} &\equiv \langle \frac{\partial \mathcal{L}_V}{\partial a_1} \rangle = v_2 \Im m(m_{12}^2 e^{i\xi}) \\
T_{a_2} &\equiv \langle \frac{\partial \mathcal{L}_V}{\partial a_2} \rangle = -v_1 \Im m(m_{12}^2 e^{i\xi})
\end{aligned}
$$

- where
  $\tan\beta = v_2/v_1 \qquad M_Z^2 = (g_w^2 + g'^2)v^2/4 \qquad v^2 = v_1^2 + v_2^2.$
- The orthogonal rotation of the CP-odd fields,

$$\begin{pmatrix} a_1 \\ a_2 \end{pmatrix} = \begin{pmatrix} \cos\beta & -\sin\beta \\ \sin\beta & \cos\beta \end{pmatrix} \begin{pmatrix} G^0 \\ a \end{pmatrix}, \qquad (2)$$

  gives rise to a flat direction in the Higgs potential with respect to the G^0 field, i.e. $\langle \partial\mathcal{L}_V/\partial G^0 \rangle = 0$.
- Newly defined basis: mass matrix of the CP-odd scalars becomes diag$(0,\ M_a^2)$
  $\Rightarrow G^0$ field becomes the Goldstone boson, which is absorbed by the longitudinal component of the Z boson.

- But, the orthogonal rotation leads to a non-trivial CP-odd tadpole parameter given by

$$T_a \equiv \langle \frac{\partial \mathcal{L}_V}{\partial a} \rangle = -v\,\Im m(m_{12}^2 e^{i\xi})$$

- At the tree level, we choose ξ such that $m_{12}^2 e^{i\xi}$ is a real number $\Rightarrow T_a = 0$.

$\Rightarrow$ CP-Conserved.

- Beyond tree level, $m_{12}^2 e^{i\xi}$ acquires a imaginary part.

$\Rightarrow$ CP-violation.

CP violation in MSSM contd.

- The mixing term :

$$\mathcal{M}^2_{SP} \;=\; -\frac{T_a}{v}\begin{pmatrix} s_\beta & c_\beta \\ -c_\beta & s_\beta \end{pmatrix} \simeq \mathcal{O}\left(\frac{m_t^4}{v^2}\frac{|\mu||A_t|}{32\pi^2 M^2_{\rm SUSY}}\right)\sin\phi_{\rm CP}$$

  where,
  $\phi_{\rm CP} = \arg(A_t\mu) + \xi \quad M^2_{\rm SUSY} = \frac{1}{2}\left(m^2_{\tilde{t}_1} + m^2_{\tilde{t}_2}\right)$
- CP-phases of gnuino mass parameter also contribute through the threshold corrections $\sim f(M^*\mu^*)$. back

Signals

No.	Signal topology	BP1	BP2	BP3
1	$n_{jet} \leq 4(b-\text{jet} \geq 3) + l \geq 2(\text{OSD} \geq 1) + \not{p}_T \leq 20$ $p_T^{j1} \leq 75 + p_T^{j2} \leq 50 + p_T^{l1} \leq 90 + p_T^{l2} \leq 90$ $p_T^{j3} \leq 40 + M_{eff} \leq 200 + \lvert M_{ll} - 90 \rvert \leq 3$	0.27	0.33	9.9
2	$n_{jet} \leq 4(b-\text{jet} = 3) + l \geq 2(\text{OSD} \geq 1) + \not{p}_T \leq 20$ $p_T^{j1} \leq 90 + p_T^{j_i(i\neq 1)} \leq 70$ $M_{eff} \leq 200 + \lvert M_{ll} - 90 \rvert \leq 3 + \phi_{j_2,l_1} \leq 1.6$	0.25	0.30	6.9
3	$n_{jet} \leq 4(b-\text{jet} = 3) + l \geq 2(\text{OSD} \geq 1) + \not{p}_T \leq 20$ $p_T^{j1} \leq 70 + p_T^{j2)} \leq 70$ $M_{eff} \leq 200 + \lvert M_{ll} - 90 \rvert \leq 2.5 + 0.5 \leq \phi_{j_2,l_1} \leq 1.8$	0.16	0.20	3.9
4	$n_{jet} \leq 4(b-\text{jet} = 3) + l \geq 2(\text{OSD} \geq 1) + \not{p}_T \leq 20$ $p_T^{j1} \leq 90 + p_T^{j2)} \leq 70$ $M_{eff} \leq 200 + \lvert M_{ll} - 90 \rvert \leq 2.5$	0.31	0.38	10.1
5	$n_{jet} \leq 3(b-\text{jet} = 3) + l \geq 2(\text{OSD} \geq 1) + \not{p}_T \leq 20$ $p_T^{j1} \leq 75 + p_T^{j2} \leq 50 + p_T^{j3} \leq 40$ $+\lvert M_{ll} - 90 \rvert \leq 2.5$	0.06	0.08	2.5

Table: Event rates for the CPX benchmark points of an integrated luminosity of 1 fb^{-1}

Backgrounds

No.	Signal topology	$t\bar{t}$	$t\bar{t}Z$	$t\bar{t}b\bar{b}$
1	$n_{jet} \leq 4(b-\mathrm{jet} \geq 3) + l \geq 2(\mathrm{OSD} \geq 1) + \not{p}_{\mathrm{T}} \leq 20$ $p_T^{j_1} \leq 75 + p_T^{j_2} \leq 50 + p_T^{l_1} \leq 90 + p_T^{l_2} \leq 90$ $p_T^{j_1} \leq 40 + M_{eff} \leq 200 + \vert M_{ll} - 90\vert \leq 3$	0.10	0.005	0.0
2	$n_{jet} \leq 4(b-\mathrm{jet} = 3) + l \geq 2(\mathrm{OSD} \geq 1) + \not{p}_{\mathrm{T}} \leq 20$ $p_T^{j_1} \leq 90 + p_T^{j_i(i\neq1)} \leq 70$ $M_{eff} \leq 200 + \vert M_{ll} - 90\vert \leq 3 + \phi_{j_2,l_1} \leq 1.6$	0.07	0.004	0.0
3	$n_{jet} \leq 4(b-\mathrm{jet} = 3) + l \geq 2(\mathrm{OSD} \geq 1) + \not{p}_{\mathrm{T}} \leq 20$ $p_T^{j_1} \leq 70 + p_T^{j_2)} \leq 70$ $M_{eff} \leq 200 + \vert M_{ll} - 90\vert \leq 2.5 + 0.5 \leq \phi_{j_2,l_1} \leq 1.8$	0.07	0.003	0.0
4	$n_{jet} \leq 4(b-\mathrm{jet} = 3) + l \geq 2(\mathrm{OSD} \geq 1) + \not{p}_{\mathrm{T}} \leq 20$ $p_T^{j_1} \leq 90 + p_T^{j_2)} \leq 70$ $M_{eff} \leq 200 + \vert M_{ll} - 90\vert \leq 2.5$	0.10	0.005	0.0
5	$n_{jet} \leq 3(b-\mathrm{jet} = 3) + l \geq 2(\mathrm{OSD} \geq 1) + \not{p}_{\mathrm{T}} \leq 20$ $p_T^{j_1} \leq 75 + p_T^{j_2} \leq 50 + p_T^{j_3} \leq 40$ $+\vert M_{ll} - 90\vert \leq 2.5$	0.04	0.001	0.0

Table: Event rates for the backgrounds for an integrated luminosity of 1 fb^{-1}